Published in final edited form as:
Mol Cancer Ther. 2011 August ; 10(8): 1470–1480. doi:10.1158/1535-7163.MCT-11-0152.

Restitution of tumor suppressor microRNAs using a systemic nanovector inhibits pancreatic cancer growth in mice

Dipankar Pramanik[1], **Nathaniel R. Campbell**[1], **Collins Karikari**[1], **Raghu Chivukula**[2], **Oliver A. Kent**[2], **Joshua T. Mendell**[2,3,4,5], and **Anirban Maitra**[1,3,6,7]

[1]The Sol Goldman Pancreatic Cancer Research Center, Johns Hopkins University School of Medicine, Baltimore, Maryland 21205, USA.

[2]Howard Hughes Medical Institute, Johns Hopkins University School of Medicine, Baltimore, Maryland 21205, USA.

[3]The McKusick-Nathans Institute of Genetic Medicine, Johns Hopkins University School of Medicine, Baltimore, Maryland 21205, USA.

[4]Department of Pediatrics, Johns Hopkins University School of Medicine, Baltimore, Maryland 21205, USA.

[5]Department of Molecular Biology and Genetics, Johns Hopkins University School of Medicine, Baltimore, Maryland 21205, USA.

[6]Department of Pathology, Johns Hopkins University School of Medicine, Baltimore, Maryland 21205, USA.

[7]Department of Oncology; Johns Hopkins University School of Medicine, Baltimore, Maryland 21205, USA.

Abstract

Misexpression of microRNAs (miRNAs) is widespread in human cancers, including in pancreatic cancer. Aberrations of miRNA include overexpression of oncogenic miRs ("Onco-miRs"), or downregulation of so-called tumor suppressor "TSG-miRs". Restitution of TSG-miRs in cancer cells through systemic delivery is a promising avenue for pancreatic cancer therapy. We have synthesized a lipid-based nanoparticle for systemic delivery of miRNA expression vectors to cancer cells ("nanovector"). The plasmid DNA-complexed nanovector is ~100nM in diameter, and demonstrates no apparent histopathological or biochemical evidence of toxicity upon intravenous injection. Two miRNA candidates known to be downregulated in the majority of pancreatic cancers were selected for nanovector delivery: miR-34a, which is a component of the p53 transcriptional network and regulates "cancer stem cell" (CSC) survival, and the miR-143/145 cluster, which together repress the expression of *KRAS2*, and its downstream effector Ras-responsive element binding protein-1 (*RREB1*). Systemic intravenous delivery with either miR-34a or miR-143/145 nanovectors inhibited the growth of MiaPaCa-2 subcutaneous xenografts ($P<0.01$ for miR-34a, $P<0.05$ for miR-143/145); the effects were even more pronounced in the orthotopic (intra-pancreatic) setting ($P<0.0005$ for either nanovector), when compared to vehicle or "mock" nanovector delivering an empty plasmid. Tumor growth inhibition was accompanied by increased apoptosis and decreased proliferation. MiRNA restitution was confirmed in treated xenografts by significant upregulation of the corresponding miRNA, and significant decreases in specific miRNA targets (SIRT1, *CD44* and *aldehyde dehydrogenase* for

Corresponding author: Anirban Maitra, MBBS, Professor of Pathology and Oncology, Johns Hopkins University School of Medicine, CRB II Room 345; 1550 Orleans St, Baltimore, MD 21231. Ph: (410) 955 3511; Fax: (410) 614 0671; amaitra1@jhmi.edu.

Conflicts of interest: The authors declare no financial conflicts of interest

miR34a, and *KRAS2* and *RREB1* for miR-143/145). The nanovector is a platform with potential broad applicability in systemic miRNA delivery to cancer cells.

Keywords

microRNA delivery; nanovector; miR-34a; miR-143/145; pancreatic cancer

Introduction

Pancreatic ductal adenocarcinoma (i.e., pancreatic cancer) is the fourth leading cause of cancer-related death, accounting for approximately 38,000 lives each year in the United States (1). The overwhelming majority of patients present with locally advanced or distant metastatic disease, rendering their cancers inoperable. Despite advances in chemotherapy and radiation therapy, the 5-year survival rate is still less than 5%, indicating the ineffectiveness of current approaches to treatment. The recent sequencing of the pancreatic cancer genome has underscored the considerable heterogeneity of somatic DNA alterations between individual tumors (2), and the challenges for molecularly targeted therapies in this neoplasm.

Micro RNAs (miRNAs) are small non-coding RNAs consisting of 18–24 nucleotides that regulate the expression of coding genes by binding imperfectly with their 3'UTR region (3). The effects of miRNAs in regulating eukaryotic transcript expression, and physiological processes such as cell proliferation, differentiation, and apoptosis have gained widespread interest in the last decade (4). More recently, the role of miRNAs in cancer pathogenesis has been studied extensively, with abnormal miRNA expression levels found in nearly all human cancers (5). Misexpression of miRNAs is not merely an epiphenomenon of the neoplastic process, but deregulated miRNAs directly contribute to altered physiological states in tumor cells. Analogous to coding genes, miRNAs are also comprised of subsets that can promote tumorigenesis ("Onco-miRs"), or those that inhibit neoplastic transformation (tumor suppressor "TSG-miRs") (6, 7). Onco-miRs are typically overxpressed in cancer cells, while TSG-miRs are downregulated compared to related non-neoplastic cell types, thus mimicking the pattern observed with most coding transcripts.

Not surprisingly, several groups (8–11), including ours (12), have cataloged miRNA abnormalities in pancreatic cancer. These studies have elucidated that, akin to other solid tumors, subsets of individual miRNAs (or corresponding miRNA "clusters") are either overexpressed (e.g., miR-21, miR-17-92, miR-196a, miR-200a/b, miR-221, etc.), or downregulated (e.g., miR-34a, miR-143/145, let-7 family, etc.) in pancreatic cancer. Identification of aberrant miRNAs in pancreatic cancer not only provides biological insights into the pathogenesis of this neoplasm (13, 14), but also forms a seedbed for establishing promising biomarkers for early detection in clinical samples (15, 16).

In light of the widespread abnormalities of miRNA expression in human cancers, modulation of deregulated miRNAs in cancer cells has also emerged as a promising therapeutic strategy (17). This concept centers around either the inhibition of overexpressed Onco-miRs, or the restitution of downregulated TSG-miRs in cancer cells. For example, specific chemically modified miRNA inhibitors known as "antagomirs" have been used to suppress the function of Onco-miRs *in vitro* and *in vivo*, resulting in the inhibition of tumor growth (18–20). On the contrary, restitution of TSG-miR function has also been utilized in recent preclinical studies with considerable success (21–25). Thus, one of the co-authors (J.T.M.) recently demonstrated that adeno-associated virus (AAV)-mediated delivery of miR-26a, whose expression is suppressed in hepatocellular carcinoma, leads to dramatic

reversal of progression in a murine model of the disease (21). Similarly, two groups have demonstrated the therapeutic efficacy of virally administered let-7 in attenuating mutant Kras-induced lung cancer progression in both xenograft and autochthonous mouse models (22, 23). In addition to adeno- and lenti-viral vectors, non-viral lipid-based strategies have recently been developed for systemic miRNA delivery, and applied successfully to lung and prostate cancer xenograft models (24, 25).

The objective of this current study was to establish the feasibility of systemic miRNA delivery to pancreatic cancer, specifically that of TSG-miRs that are commonly downregulated in this disease. We have selected two candidates, miR-34a and the miR-143/145 cluster, whose expression is lost in the majority of pancreatic cancer samples (12, 26, 27). Of note, expression of both miR-34a and the miR-143/145 cluster is also attenuated in the most common subtypes of human cancer, such as non-small cell, prostate, and colorectal cancers, amongst others (24, 25, 28), thus broadening the applicability of this approach beyond pancreatic cancer. We have synthesized a lipid-based nanoparticle for systemic delivery of miRNA expression vectors to cancer cells ("nanovector"), and demonstrated the significant therapeutic efficacy of restituting either miR-34a or miR-143/145 expression in subcutaneous and orthotopic pancreatic cancer xenograft models. We also confirm the lack of demonstrable toxicity in mice from the nanovector alone. Our non-viral gene delivery platform provides a prototype for safe and efficient delivery of miRNA expression vectors to cancer cells, and could be widely utilized in the preclinical, and eventually, clinical arenas.

Materials and Methods

Materials

1,2-dioleoyl-3-trimethylammonium-propane (chloride salt) (DOTAP) and 1,2-dioleoyl-sn-glycero-3-phosphoethanolamine-N-[methoxy(polyethyleneglycol)-2000] (ammonium salt) (DSPE-PEG-OMe) were purchased from Avanti Polar Lipids (Alabaster, Alabama, USA). Cell culture grade cholesterol was purchased from Sigma Aldrich (St. Louis, Missouri, USA). The MiaPaCa-2 cell line was obtained from the American Type Culture Collection (ATCC, Manassas, Virginia, USA) and cells were cultured in RPMI 1640 medium supplemented with 10% FBS and pen/strep. ATCC uses DNA fingerprinting (microsatellite analysis) for cell line authentication. CD-1 male athymic *nu/nu* mice (4–6 weeks old) were procured from Harlan (Frederick, Maryland, USA).

MicroRNA expression constructs

The miR-143/145 cluster and miR-34a were amplified from genomic DNA using *Pfu* polymerase and cloned into the XhoI site in the pMSCV-puro expression construct (Clontech Laboratories, Mountain View, California, USA). The primers for the miR-143/145 and miR-34a sequences have been previously described (26, 27). The sequences of the amplified products were confirmed by sequencing.

Preparation of lipid-based nanovector for systemic miRNA delivery

Liposomal nanoparticles were prepared by dissolving cationic amphiphile (DOTAP) and co-lipids (cholesterol and DSPE-PEG-OMe) in a 1:1:0.2 ratio, respectively, in a mixture of chloroform and methanol in a glass vial. The organic solvent was removed with a gentle flow of moisture-free nitrogen and the remaining dried film of lipid was then kept under high vacuum for 8 hours. Distilled water (*in vitro*) or 5% glucose (*in vivo*) was added to the vacuum-dried lipid film and the mixture was allowed to hydrate overnight. The vial was vortexed for 2–3 minutes at room temperature, and occasionally shaken in a 45 °C water bath to produce multilamellar vesicles (MLV). Small unilamellar vesicles (SUV) were

prepared by sonication of the MLV placed in an ice bath for 3–4 min until clarity using a Branson 450 sonifier (Danbury, Connecticut, USA) at 100% duty cycle and 25 W output power. The nanovector represents an electrostatic complex of positively charged liposomal nanoparticle and negatively charged plasmid DNA, and was prepared by mixing pMSCV-puro vectors expressing corresponding miRNAs and liposome on a charge ratio basis. Two independent miRNA nanovectors were engineered: the first delivering miR-34a, and the second delivering miR-143/145. For *in vivo* experiments, each mouse received 50 micrograms of DNA complexed with liposome at a 4:1 lipid/DNA charge ratio via tail-vein injection (*see below*).

In vitro transfection efficiency assay

The *in vitro* transfection efficiency of the nanovector platform was assessed using a firefly luciferase expression vector on a plasmid backbone. MiaPaCa-2 cells were seeded at a density of 12,000 per well in a 96-well plate 18–24 hours before transfection. Plasmid DNA (0.3μg, 0.9nmol) was complexed with varying amounts of lipids (1 to 8nmol) in serum free medium (total volume up to 100μL) for 30 minutes. The charge ratios were varied from 1:1 to 8:1 over these ranges of lipid concentration. Immediately prior to transfection, cells plated in the 96-well plate were washed with PBS (2 × 100μL) followed by the addition of nanovector. After 4 hours of incubation, the medium was replaced with fresh complete medium containing 10% FBS. The luciferase reporter gene activity was estimated after 48 hours. The cells were washed twice with PBS (100μL each) and lysed in lysis buffer (50μL). Firefly luciferase assay was performed in a Wallac Victor 2 (Perkin Elmer, Waltham, Massachusetts, USA), using 25μL injections. Total protein concentration in each well was determined by the modified Lowry method and the luciferase activity was expressed as the relative light unit (RLU) per mg of the protein. Lipofectamine 2000 (Invitrogen, Carlsbad, California, USA) was used as a positive control for transfection in this experiment. Each transfection experiment was repeated twice on two different days, and reported as average values ± standard deviation obtained for the entire series.

In vitro GFP Transfection

MiaPaCa-2 cells were seeded at a density of 48,000 per well in a 24-well plate 48 hours before transfection. Plasmid DNA (1 μg/well, pEGFP-C1, Clontech, cat. # 6084-1) was complexed with nanovector (1:1 charge ratio) in opti-MEM. The resultant pEGFP-nanovector was added to MiaPaCa-2 cells growing in complete media. After 4 hours growth media was aspirated and replaced with fresh complete media. Cells were allowed to grow for 48 hours at which point fluorescence images were taken on the FITC channel.

Nanovector toxicity study

Male CD-1 mice (Harlan Laboratory) were injected intravenously with either 5% glucose as vehicle or miR-143/145 nanovector three times per week for two weeks. Blood was collected at necropsy via cardiac puncture. Blood chemistry and renal and liver function parameters were measured by the Johns Hopkins Phenotyping Core facility (http://www.hopkinsmedicine.org/mcp/PHENOCORE/).

Xenograft Studies

All small animal (CD-1 athymic mice) experiments described conformed to the guidelines of the Animal Care and Use Committee of Johns Hopkins University. Mice were maintained in accordance with the guidelines of the American Association of Laboratory Animal Care.

Systemic delivery of miRNA nanovectors to subcutaneous pancreatic cancer xenografts

As stated above, we generated two independent miRNA nanovectors, the first delivering miR-34a, and the second delivering miR-143/145, and each was tested independently in subcutaneous and orthotopic pancreatic cancer xenograft models. To generate subcutaneous xenografts, 5×10^6 MiaPaCa-2 cells suspended in a total volume of 200 μL [PBS/Matrigel (BD Biosciences), 1:1 (v/v), prechilled to 4°C] were injected into the flanks of 5- to 6-week old male *nu/nu* mice. One week after the injection of tumor cells, subcutaneous tumor volumes (*V*) were measured with digital calipers (Fisher Scientific, Pittsburgh, Pennsylvania, USA) and calculated using the formula $V = ½(ab^2)$, where *a* is the biggest and *b* is the smallest orthogonal tumor diameter (29). Fifteen mice with successfully engrafted MiaPaCa-2 xenografts were then randomized into three cohorts of five animals each and administered one the following regimens via tail-vein injection: (a) vehicle, (b) “mock” nanovector (nanovector complexed with pMSCV alone), and (c) miR-34a nanovector, with each regimen administered three times per week for three weeks. A second series of experiments was conducted using subcutaneous MiaPaCa-2 xenografts administered either (a) vehicle or (b) miR-143/145 nanovector (five mice per arm), with the identical dosing schedule (the “mock” nanovector arm was not included based on results from the miR-34a study, *see below*). Tumor size and body weight were measured once weekly. At the culmination of treatment, visceral organs and tumor tissues were harvested, and either preserved in 10% neutral buffered formalin for histology and immunohistochemical studies, or snap frozen for nucleic acid analysis.

Systemic delivery of miRNA nanovectors to orthotopic pancreatic cancer xenografts

The generation of orthotopic human pancreatic cancer xenografts by surgical implantation in athymic mice has been described previously our group (29, 30). Briefly, freshly harvested subcutaneous MiaPaCa-2 xenografts were minced into 1 mm^3 cubes under sterile conditions for orthotopic implantation. A small pocket was prepared inside the pancreas, into which one of the previously prepared fresh tumor chunks was inserted. Two weeks after surgical orthotopic implantation, the presence of “primary” tumors was confirmed by ultrasound (Vevo660, VisualSonics, Toronto, Ontario, Canada) and measured in three orthogonal axes, *a*, *b*, and *c*; tumor volumes were determined as $V = (abc)/2$, as described (29, 30). Twenty mice with successfully engrafted MiaPaCa-2 xenografts were then randomized into four cohorts of five animals each and administered one of the following regimens by tail-vein injection: (a) 5% glucose as vehicle, (b) void nanovector, (c) miR-34a nanovector, and (d) miR-143/145 nanovector, each at three times per week for three weeks. At the culmination of therapy, visceral organs and tumor tissues were harvested and preserved in 10% neutral buffered formalin for histological studies. Additionally, tumor tissues were snap-frozen for nucleic acid analysis.

Quantitative assessment of miRNA restitution upon nanovector therapy

Total miRNA from snap-frozen MiaPaCa-2 xenografts was isolated using the mirVANA™ PARIS™ RNA isolation kit (Applied Biosystems, Carlsbad, California, USA) following the manufacturer's instructions. Thereafter, 10ng of RNA was reverse transcribed with a miRNA Reverse Transcription Kit (Applied Biosystems) using miR-34a, miR-143, and miR-145 specific RT-primers (TaqMan miRNA Assay, Applied Biosystems), as described (12, 26, 27). Quatitative PCR was performed using RNU6B or RNU44 as housekeeping control, and relative expression levels were calculated using the $2^{-\Delta\Delta Ct}$ method (31).

Quantitative assessment of miRNA targets upon nanovector therapy

Total RNA (>200 bp) was isolated from snap-frozen MiaPaCa-2 xenografts using the RNeasy Mini Kit (Qiagen, Valencia, California, USA) following the manufacturer’s

instructions. Thereafter, cDNA was generated using the High Capacity cDNA RT Kit (Applied Biosystems) with random primers. For the miR-143/145 nanovector-treated xenografts, quantitative PCR for expression of *KRAS2* and *RREB1* transcripts was performed, as previously described (26). Recent data has also shown that miR-34a re-expression depletes tumor initiating cells in pancreatic and prostate cancers (25, 32); therefore, expression of two credentialed markers of tumor initiating cells in pancreatic cancer – *CD44* and *aldehyde dehydrogenase* (*ALDH*) (33, 34) – was determined by qRT-PCR in the miR-34a nanovector-treated xenografts.

Western blot for SIRT1 expression

Tissues were harvested with RIPA buffer and protein (50μg) was loaded and separated on 4–20% SDS-polyacrylamide gradient gel. Proteins were transferred onto nitrocellulose membrane (Hybond-ECL, GE healthcare, Piscataway, New Jersey, USA) and blocked for 1 h with 5% non-fat milk in PBS containing 0.5% Tween-20 (PBS-T). Blots were then incubated with anti-silent information regulator-1 (SIRT1) antibody (1:500 dilution) for 2 hours at room temperature, followed by incubation with secondary antibody conjugated to HRP at a 1:5,000 dilution for 1 hour. After washing with PBS-T (3 × 10mL, 5 minutes each), the chemiluminescence film was developed after addition of the substrate. Anti-tubulin antibody (dilution of 1:2,000) was used as an internal control for protein loading.

Immunohistochemical analysis of RREB1 expression

Immunohistochemistry for RREB1 was performed on formalin-fixed paraffin-embedded xenograft tissues from three independent tumor samples in each cohort (control *versus* treatment), using a standard technique (29, 30). Briefly, tissues were deparaffinized in xylenes, and hydrated by a graded series of ethanol washes and pure water. Slides were incubated in 0.3% H_2O_2 in MeOH for 20 min, followed by antigen retrieval in a steamer in EDTA buffer (pH 8.0) at 90+ °C for 35 min. Sections were blocked with Dako Protein Block Serum-Free for 10 minutes at room temperature. Slides were incubated with RREB1 antibody (1:200 dilution, Abcam, rabbit polyclonal, cat. # ab64168) in Normal Antibody Diluent (ScyTek, phosphate buffered) for 1 hour at room temperature. Slides were then post-blocked in PowerVision Post-Blocking for 10 minutes at room temperature and incubated with appropriate PowerVision+ Poly-HRP conjugated antibody for 20 minutes at room temperature. The reaction was developed using DAB+ (Leica Microsystems, cat. # PV6126), and counterstained with hematoxylin. Relative intensity of staining was evaluated by a pathologist (A.M.) blinded to the arms.

Assessment of proliferation (Ki-67 immunohistochemistry) and apoptosis (TUNEL)

Immunohistochemistry for proliferation (Ki-67 antigen) was performed on formalin-fixed paraffin-embedded xenograft tissues, as previously described (29, 30), using an anti-MIB-1 (Ki-67) antibody (clone K2, dilution 1:100, Ventana Medical Systems, Tucson, Arizona, USA). TUNEL assay for apoptosis was performed according to manufacturer protocol (DeadEnd™ Fluorometric TUNEL System, Promega).

Results

In vitro and in vivo characterization of nanovectors for systemic miRNA delivery

To begin, we synthesized a liposomal nanoparticle through rehydration of a thin layer of DOTAP, cholesterol, and DSPE-PEG-OMe, in a 1:1:0.02 molar ratio. The resultant aqueous suspension of cationic liposomes could undergo complex formation with plasmid DNA to form a "nanovector". The use of such a liposomal nanovector was based upon the established safety and efficacy of such formulations, and the enhanced circulation stability

afforded by the presence of polyethylene glycol (35). When evaluated by transmission electron microscopy (TEM), the nanovector with therapeutic cargo was found to have an average diameter in the range of ~100 nm (Figure 1a). We next evaluated the *in vitro* transfection efficiency of the nanovector in MiaPaCa-2 cells, using a firefly luciferase reporter assay and EGFP fluorescence microscopy. The transfection efficiency of the nanovector with a 4:1 lipid/DNA charge-ratio was comparable to that of Lipofectamine 2000 as positive control (Figure 1b). Additionally, visualization of cells transfected with EFGP-expressing vector indicated effective localization of the DNA cargo to cells *in vitro* (Figure 1c). Next, we evaluated the potential for adverse effects upon systemic nanovector therapy by measuring a panel of hematological and biochemical parameters in non-tumor bearing CD-1 mice that had received either buffer (5% glucose) or miR-143/145 nanovector by tail-vein injection, three times weekly for two weeks. Compared to mice treated intravenously with buffer, we observed no significant differences in any of the examined laboratory parameters, including hematology, and liver and renal function tests (Supplementary Figure 1), underscoring the relative safety of this delivery platform.

Systemic miRNA delivery with nanovectors inhibits the growth of subcutaneous pancreatic cancer xenografts

We next moved to evaluating whether restitution of miRNA could inhibit pancreatic cancer growth in a subcutaneous xenograft model. Successfully engrafted MiaPaCa-2 xenografts were treated via tail vein injection with either vehicle, "mock" nanovector, miR-34a nanovector, or mR-143/145 nanovector three times weekly, for three weeks. Significant tumor growth inhibition was observed when mice were treated with either miR-34a or miR-143/145 nanovectors, as compared to "mock" and vehicle controls (Figures 2a and 2b). Also of note, the effects of the "mock" nanovector were essentially identical to vehicle-only treated xenografts, indicating that the growth-inhibitory effects were caused by the expression of the target miRNAs. Examination of H&E stained sections of treated xenografts demonstrated confluent sheets of necrosis in both miR-34a and miR-143/145 arms, compared to the vehicle and "mock" nanovector cohorts (Figure 2c). This observation was confirmed by TUNEL assessment for fragmented DNA (Figure 2d), which indicated more widespread apoptosis in treated tumors than in the vehicle and "mock" controls.

Systemic miRNA delivery with nanovectors inhibits the growth of orthotopic pancreatic cancer xenografts

Although such subcutaneous xenografts provided a preliminary indication of the efficacy of miRNA restitution, they fail to recapitulate many key aspects of the tumor microenvironment. To overcome some of these limitations, including drug distribution kinetics observed in the pancreas, an intrapancreatic orthotopic xenograft is considered to be more biologically relevant (36, 37). We therefore investigated the efficacy of restitution of miR-34a and miR-143/145 in an orthotopic MiaPaCa-2 pancreatic cancer xenograft model. As shown in Figure 3a, the growth of orthotopic xenografts was significantly inhibited by restitution of either miR-34a or miR-143/145 through systemic nanovector delivery, compared to vehicle and "mock" nanovector arms. Subsequent histological analysis confirmed confluent sheets of necrosis in the miRNA nanovector arms, similar to what was observed in the subcutaneous milieu (Figure 3b), a trend reiterated by TUNEL staining for apoptosis (Figure 3c). Further, to measure whether miRNA restitution also impacted proliferation, we performed immunohistochemical staining for Ki-67 and observed strikingly reduced nuclear Ki-67 levels in both treatment groups (Figure 3d).

Systemic nanovector therapy modulates miRNA targets in pancreatic cancer xenografts

To confirm that the miRNA-delivering nanovectors were successfully reaching the tumor tissue, we measured the levels of mature miRNA in subcutaneous MiaPaCa-2 xenografts by

qRT-PCR. Using miRNA-specific primers, we established significant increases in the expression levels of respective miRNAs in xenografts treated with either of the two nanovectors, compared to vehicle control (Figure 4a, $P = 0.04$ for miR-34a; $P = 0.03$ for miR-143; and $P = 0.001$ for miR-145). To validate the effects of miRNA restitution, we analyzed expression levels of key targets of miR34a, miR-143, and miR145, following systemic therapy. For example, silent information regulator-1 (SIRT1) is a class III histone deacetylase that regulates apoptosis in response to various oxidative and genotoxic stress (38). SIRT1 expression is repressed by miR-34a binding to its 3'UTR seed sequence, establishing SIRT1 as a direct target of miR-34a (39). We observed a marked decrease in SIRT1 levels in miR-34a nanovector-treated xenografts as compared to vehicle control (Figure 4b), indicating a tangible pharmacodynamic readout of miRNA delivery. Multiple lines of evidence also point to the role of miR-34a repression in the expansion of tumor initiating cells (i.e. "cancer stem cells"), and that restitution of miR-34a expression depletes this subpopulation in cancers (25, 32). Therefore, expression of two credentialed markers of tumor initiating cells in pancreatic cancer – *CD44* and *aldehyde dehydrogenase* (*ALDH*) (33, 34) – was determined by qRT-PCR in the miR-34a nanovector-treated xenografts, with both demonstrating a significant reduction (Figure 4c, $P = 0.01$ for *ALDH* and $P = 0.05$ for *CD44*).

Recently the repression of miR-143 and miR-145 by oncogenic Ras was identified by our group as a new tumor-promoting feed-forward pathway (26). Kras, through its downstream effector Ras-responsive element binding protein-1 (RREB1), represses the transcription of the miR-143/145 cluster, with RREB1 binding to the promoter element of the miRNA primary transcript. In turn, mature miR-143 and miR-145 repress *KRAS2* and *RREB1*, respectively, effectively completing the loop. Therefore, restitution of miR-143/145 expression in MiaPaCa-2 xenografts should attenuate expression of both *KRAS2* and *RREB1*. Expectedly, we observed significant downregulation of both transcripts ($P = 0.001$) in xenografts treated with miR-143/145 nanovector compared with controls (Figure 4d, ***left***). Additionally, resultant downregulation of RREB1 protein expression could be observed through immunohistochemical staining of tumor sections from both miR-143/145 nanovector-treated and vehicle control xenografts (Figure 4d, ***right***). This serves as important *in vivo* confirmation of the aforementioned feed-forward pathway, and indicates that treatment with the systemic miR-143/145 nanovector results in restitution of mature miR-143 and miR-145, with downregulation of *KRAS2/RREB1* targets accompanying the observed tumor growth inhibition.

Discussion

In this study, we have shown that systemic delivery of TSG-miRs using a nanovector delivery platform can inhibit the growth of pancreatic cancer xenografts in both subcutaneous and orthotopic milieus. Most molecularly targeted therapeutic approaches are directed towards blocking aberrant hyperfunction of oncogenic components; however, the current miRNA delivery strategy is geared towards regaining function lost specifically in cancer cells.

We selected two miRNA candidates for systemic delivery in pancreatic cancer models: miR-34a and the miR-143/145 cluster. As data from our group and others have established (8, 10, 12, 26, 27), these miRs are downregulated (or completely absent) in the majority of pancreatic cancers. Functionally, miR-34a is a component of the p53 transcriptional network and its loss in cancer cells is associated with resistance to apoptosis induced by p53 activating agents (27, 40, 41). In cancer cells with wild type p53, ectopic expression of miR-34a levels can restore p53 function by repressing the deacetylase SIRT1, thereby enhancing levels of active (acetylated) p53 (42). The repertoire of miR-34a targets are

expectedly quite diverse, and include molecules involved in promoting cellular proliferation (cyclin D1, cyclin-dependent kinases CDK4 and 6) and blocking apoptosis (Bcl-2) (43–45). Thus, restoring miR-34a function in cancer cells is expected to have both pro-apoptotic and anti-proliferative effects, as was observed in the miR-34a nanovector-treated xenografts by TUNEL and Ki-67 labeling, respectively. Recently, miR-34a has also been implicated in regulating the number and function of tumor-initiating cells (i.e. "cancer stem cells" or CSCs) in solid cancers (25, 32). Specifically, studies in pancreatic and prostate cancer models have demonstrated that CSCs in these cancer types harbor low miR-34a levels, while re-expression of this miRNA significantly decreases CSC clonogenicity and survival, and tumor engraftment capacity *in vivo*. In pancreatic cancer, these profound deleterious effects on CSCs are observed irrespective of p53 functional status (32), underscoring the applicability of therapeutic miR-34a restitution to a disease that harbors *TP53* mutations in approximately 70% of cases (2). Indeed, using two credentialed surrogate measures of pancreatic cancer CSCs, *ALDH* and *CD44* (33, 34), we demonstrated a significant downregulation in expression of both transcripts in miR-34a nanovector-treated xenografts. Finally, given the widespread loss of expression of miR-34a in many other solid cancers (39, 44, 46), there is also compelling rationale to test the efficacy of the nanovector platform in corresponding preclinical disease models.

The second candidate we tested using nanovector delivery is a cluster of two co-transcribed miRNAs, miR-143/145, whose expression is also frequently lost in many solid and hematological malignancies, including colorectal cancers where a consistent downregulation was first identified (47). Our recent work has identified the existence of a feed-forward loop in pancreatic cancer cells, wherein the Ras effector protein RREB1 directly represses the expression of miR-143/145, thereby relieving the miRNA-mediated repression of *KRAS2* and *RREB1* transcripts (26). Not unexpectedly, the robust tumor growth inhibition observed *in vivo* with miR-143/145 nanovector therapy is accompanied by significant downregulation in *KRAS2* and *RREB1* transcripts, as well as decreased RREB1 protein expression by immunohistochemistry. The seminal importance of the *KRAS2* oncogene to pancreatic cancer cannot be overstated - somatic activating mutations are found in greater than 90% of cases, and Ras is implicated in both tumor initiation and tumor maintenance (1, 48). Nonetheless, pharmacological blockade of this small GTPase protein has been challenging, as small molecule inhibitors of Ras farnesylation have failed to improve median survival in clinical trials (49). The miR-143/145 nanovector represents a tangible genetic approach towards direct inhibition of *KRAS2* in pancreatic cancer, and future studies in the Ras-driven genetically engineered models of pancreatic cancer (50) will provide additional insights on the therapeutic potential of this modality in an autochthonous setting.

We performed two independent experiments using TSG-miRs (i.e. "miRNA monotherapy"), each of which demonstrated significant and comparable tumor growth inhibition *in vivo*. We are currently developing delivery methods for concurrent restitution of two or more diverse TSG miRs targeting non-overlapping coding genes (i.e., "miRNA combination therapy"), with the intent of achieving therapeutic synergy. This approach is based on either the concurrent administration of two independent nanovectors (for example, miR-34a or miR-143/145 nanovectors illustrated in this study), or the generation of a single nanovector capable of delivering dual therapeutic cargo (such as a bi-cistronic vector expressing two miRNAs simultaneously). Additionally, combination therapy with other traditional chemotherapy agents (e.g., gemcitabine) may yield improved effects in pancreatic cancer. The lack of demonstrable adverse effects at the histological or biochemical level is encouraging and likely because saturation of endogenous levels of miR-34a and miR-143/145 are already achieved in normal cells. Thus, to conclude, the nanovector platform we have designed can be used for systemic delivery of TSG miRNAs to cancer cells. Although the proof-of-principle studies presented here utilize pancreatic cancer as a

disease model, it is conceivable that this approach will be broadly applicable across other tumor types, delivering potentially any TSG miR that is a candidate for restitution in cancer cells.

Supplementary Material

Refer to Web version on PubMed Central for supplementary material.

Acknowledgments

Supported by the Sol Goldman Pancreatic Cancer Research Center, the Michael Rolfe Foundation for Pancreatic Cancer Research; NIH R01CA113669; NIH P01CA134292; NIH U54CA151838; and the Flight Attendants Medical Research Institute.

References

1. Maitra A, Hruban RH. Pancreatic cancer. Annu Rev Pathol. 2008; 3:157–188. [PubMed: 18039136]
2. Jones S, Zhang X, Parsons DW, et al. Core signaling pathways in human pancreatic cancers revealed by global genomic analyses. Science. 2008; 321:1801–1806. [PubMed: 18772397]
3. Chang TC, Mendell JT. The Roles of microRNAs in Vertebrate Physiology and Human Disease. Annu Rev Genomics Hum Genet. 2007
4. Carthew RW, Sontheimer EJ. Origins and Mechanisms of miRNAs and siRNAs. Cell. 2009; 136:642–655. [PubMed: 19239886]
5. Garzon R, Calin GA, Croce CM. MicroRNAs in Cancer. Annu Rev Med. 2009; 60:167–179. [PubMed: 19630570]
6. Cho WC. OncomiRs: the discovery and progress of microRNAs in cancers. Mol Cancer. 2007; 6:60. [PubMed: 17894887]
7. Garofalo M, Condorelli G, Croce CM. MicroRNAs in diseases and drug response. Curr Opin Pharmacol. 2008; 8:661–667. [PubMed: 18619557]
8. Bloomston M, Frankel WL, Petrocca F, Volinia S, Alder H, Hagan JP, et al. MicroRNA expression patterns to differentiate pancreatic adenocarcinoma from normal pancreas and chronic pancreatitis. Jama. 2007; 297:1901–1908. [PubMed: 17473300]
9. Lee EJ, Gusev Y, Jiang J, Nuovo GJ, Lerner MR, Frankel WL, et al. Expression profiling identifies microRNA signature in pancreatic cancer. Int J Cancer. 2007; 120:1046–1054. [PubMed: 17149698]
10. Szafranska AE, Davison TS, John J, Cannon T, Sipos B, Maghnoouj A, et al. MicroRNA expression alterations are linked to tumorigenesis and non-neoplastic processes in pancreatic ductal adenocarcinoma. Oncogene. 2007; 26:4442–4452. [PubMed: 17237814]
11. Zhang Y, Li M, Wang H, Fisher WE, Lin PH, Yao Q, et al. Profiling of 95 MicroRNAs in Pancreatic Cancer Cell Lines and Surgical Specimens by Real-Time PCR Analysis. World J Surg. 2009; 33:698–709. [PubMed: 19030927]
12. Kent OA, Mullendore M, Wentzel EA, Lopez-Romero P, Tan AC, Alvarez H, et al. A resource for analysis of microRNA expression and function in pancreatic ductal adenocarcinoma cells. Cancer biology & therapy. 2009; 8:2013–2024. [PubMed: 20037478]
13. Volinia S, Calin GA, Liu CG, Ambs S, Cimmino A, Petrocca F, et al. A microRNA expression signature of human solid tumors defines cancer gene targets. Proc Natl Acad Sci U S A. 2006; 103:2257–2261. [PubMed: 16461460]
14. Gironella M, Seux M, Xie MJ, Cano C, Tomascini R, Gommeaux J, et al. Tumor protein 53-induced nuclear protein 1 expression is repressed by miR-155, and its restoration inhibits pancreatic tumor development. Proc Natl Acad Sci U S A. 2007; 104:16170–16175. [PubMed: 17911264]
15. Habbe N, Koorstra JB, Mendell JT, Offerhaus GJ, Ryu JK, Feldmann G, et al. MicroRNA miR-155 is a biomarker of early pancreatic neoplasia. Cancer biology & therapy. 2009; 8

16. Szafranska AE, Doleshal M, Edmunds HS, Gordon S, Luttges J, Munding JB, et al. Analysis of microRNAs in pancreatic fine-needle aspirates can classify benign and malignant tissues. Clin Chem. 2008; 54:1716–1724. [PubMed: 18719196]

17. Garzon R, Marcucci G, Croce CM. Targeting microRNAs in cancer: rationale, strategies and challenges. Nat Rev Drug Discov. 9:775–789. [PubMed: 20885409]

18. Ma L, Reinhardt F, Pan E, Soutschek J, Bhat B, Marcusson EG, et al. Therapeutic silencing of miR-10b inhibits metastasis in a mouse mammary tumor model. Nature biotechnology. 28:341–347.

19. Felicetti F, Errico MC, Bottero L, Segnalini P, Stoppacciaro A, Biffoni M, et al. The promyelocytic leukemia zinc finger-microRNA-221/-222 pathway controls melanoma progression through multiple oncogenic mechanisms. Cancer research. 2008; 68:2745–2754. [PubMed: 18417445]

20. Fontana L, Fiori ME, Albini S, Cifaldi L, Giovinazzi S, Forloni M, et al. Antagomir-17-5p abolishes the growth of therapy-resistant neuroblastoma through p21 and BIM. PLoS One. 2008; 3:e2236. [PubMed: 18493594]

21. Kota J, Chivukula RR, O'Donnell KA, Wenztel EA, Montgomery CL, Hwang HW, et al. Therapeutic microRNA delivery suppresses tumorigenesis in a murine liver cancer model. Cell. 2009; 137:1005–1017. [PubMed: 19524505]

22. Esquela-Kerscher A, Trang P, Wiggins JF, Patrawala L, Cheng A, Ford L, et al. The let-7 microRNA reduces tumor growth in mouse models of lung cancer. Cell Cycle. 2008; 7:759–764. [PubMed: 18344688]

23. Kumar MS, Erkeland SJ, Pester RE, Chen CY, Ebert MS, Sharp PA, et al. Suppression of non-small cell lung tumor development by the let-7 microRNA family. Proc Natl Acad Sci U S A. 2008; 105:3903–3908. [PubMed: 18308936]

24. Wiggins JF, Ruffino L, Kelnar K, Omotola M, Patrawala L, Brown D, et al. Development of a lung cancer therapeutic based on the tumor suppressor microRNA-34. Cancer research. 70:5923–5930. [PubMed: 20570894]

25. Liu C, Kelnar K, Liu B, Chen X, Calhoun-Davis T, Li H, et al. The microRNA miR-34a inhibits prostate cancer stem cells and metastasis by directly repressing CD44. Nat Med.

26. Kent OA, Chivukula RR, Mullendore M, Wentzel EA, Feldmann G, Lee KH, et al. Repression of the miR-143/145 cluster by oncogenic Ras initiates a tumor-promoting feed-forward pathway. Genes Dev. 24:2754–2759. [PubMed: 21159816]

27. Chang TC, Wentzel EA, Kent OA, Ramachandran K, Mullendore M, Lee KH, et al. Transactivation of miR-34a by p53 broadly influences gene expression and promotes apoptosis. Mol Cell. 2007; 26:745–752. [PubMed: 17540599]

28. Tazawa H, Tsuchiya N, Izumiya M, Nakagama H. Tumor-suppressive miR-34a induces senescence-like growth arrest through modulation of the E2F pathway in human colon cancer cells. Proc Natl Acad Sci U S A. 2007; 104:15472–15477. [PubMed: 17875987]

29. Feldmann G, Dhara S, Fendrich V, Bedja D, Beaty R, Mullendore M, et al. Blockade of hedgehog signaling inhibits pancreatic cancer invasion and metastases: a new paradigm for combination therapy in solid cancers. Cancer research. 2007; 67:2187–2196. [PubMed: 17332349]

30. Feldmann G, Fendrich V, McGovern K, Bedja D, Bisht S, Alvarez H, et al. An orally bioavailable small-molecule inhibitor of Hedgehog signaling inhibits tumor initiation and metastasis in pancreatic cancer. Mol Cancer Ther. 2008; 7:2725–2735. [PubMed: 18790753]

31. Schmittgen TD, Livak KJ. Analyzing real-time PCR data by the comparative C(T) method. Nat Protoc. 2008; 3:1101–1108. [PubMed: 18546601]

32. Ji Q, Hao X, Zhang M, Tang M, Yang M, Li L, et al. MicroRNA miR-34 inhibits human pancreatic cancer tumor-initiating cells. PLoS One. 2009; 4:e6816. [PubMed: 19714243]

33. Li C, Heidt DG, Dalerba P, Burant CF, Zhang L, Adsay V, et al. Identification of pancreatic cancer stem cells. Cancer research. 2007; 67:1030–1037. [PubMed: 17283135]

34. Rasheed ZA, Yang J, Wang Q, Kowalski J, Freed I, Murter C, et al. Prognostic significance of tumorigenic cells with mesenchymal features in pancreatic adenocarcinoma. Journal of the National Cancer Institute. 102:340–351. [PubMed: 20164446]

35. Karmali PP, Chaudhuri A. Cationic liposomes as non-viral carriers of gene medicines: Resolved issues, open questions, and future promises. Medicinal Research Reviews. 2007; 27:696–722. [PubMed: 17022036]
36. Kerbel RS. Human tumor xenografts as predictive preclinical models for anticancer drug activity in humans: better than commonly perceived-but they can be improved. Cancer biology & therapy. 2003; 2:S134–S139. [PubMed: 14508091]
37. Hoffman RM. Orthotopic metastatic mouse models for anticancer drug discovery and evaluation: a bridge to the clinic. Invest New Drugs. 1999; 17:343–359. [PubMed: 10759402]
38. Herranz D, Serrano M. SIRT1: recent lessons from mouse models. Nature reviews. 10:819–823.
39. Yamakuchi M, Ferlito M, Lowenstein CJ. miR-34a repression of SIRT1 regulates apoptosis. Proc Natl Acad Sci U S A. 2008; 105:13421–13426. [PubMed: 18755897]
40. Hermeking H. The miR-34 family in cancer and apoptosis. Cell Death Differ. 17:193–199. [PubMed: 19461653]
41. He X, He L, Hannon GJ. The guardian's little helper: microRNAs in the p53 tumor suppressor network. Cancer research. 2007; 67:11099–11101. [PubMed: 18056431]
42. Yamakuchi M, Lowenstein CJ. MiR-34, SIRT1 and p53: the feedback loop. Cell Cycle. 2009; 8:712–715. [PubMed: 19221490]
43. Tarasov V, Jung P, Verdoodt B, Lodygin D, Epanchintsev A, Menssen A, et al. Differential regulation of microRNAs by p53 revealed by massively parallel sequencing: miR-34a is a p53 target that induces apoptosis and G1-arrest. Cell Cycle. 2007; 6:1586–1593. [PubMed: 17554199]
44. Li Y, Guessous F, Zhang Y, Dipierro C, Kefas B, Johnson E, et al. MicroRNA-34a inhibits glioblastoma growth by targeting multiple oncogenes. Cancer research. 2009; 69:7569–7576. [PubMed: 19773441]
45. Sun F, Fu H, Liu Q, Tie Y, Zhu J, Xing R, et al. Downregulation of CCND1 and CDK6 by miR-34a induces cell cycle arrest. FEBS Lett. 2008; 582:1564–1568. [PubMed: 18406353]
46. Stallings RL. MicroRNA involvement in the pathogenesis of neuroblastoma: potential for microRNA mediated therapeutics. Curr Pharm Des. 2009; 15:456–462. [PubMed: 19199973]
47. Michael MZ, SM OC, van Holst Pellekaan NG, Young GP, James RJ. Reduced accumulation of specific microRNAs in colorectal neoplasia. Mol Cancer Res. 2003; 1:882–891. [PubMed: 14573789]
48. Hingorani SR, Tuveson DA. Ras redux: rethinking how and where Ras acts. Curr Opin Genet Dev. 2003; 13:6–13. [PubMed: 12573429]
49. Van Cutsem E, van de Velde H, Karasek P, Oettle H, Vervenne WL, Szawlowski A, et al. Phase III trial of gemcitabine plus tipifarnib compared with gemcitabine plus placebo in advanced pancreatic cancer. J Clin Oncol. 2004; 22:1430–1438. [PubMed: 15084616]
50. Olive KP, Tuveson DA. The use of targeted mouse models for preclinical testing of novel cancer therapeutics. Clin Cancer Res. 2006; 12:5277–5287. [PubMed: 17000660]

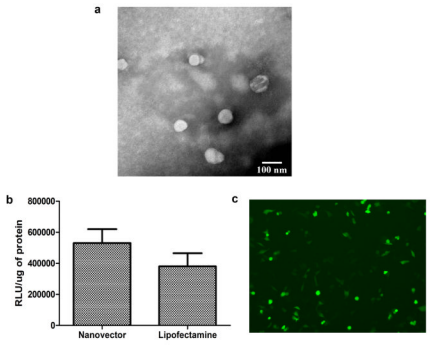

Figure 1. Size determination and transfection efficiency of DNA-loaded nanovector

(a) Transmission electron microscopy (TEM) image of DNA loaded nanovector, measuring an average 81±12nM in diameter.

(b) MiaPaCa-2 cells were transfected with nanovectors containing firefly luciferase expression vector. Relative luciferase units are compared against those obtained with using Lipofectamine 2000 as positive control.

(c) *In vitro* transfection of pEGFP-C1 plasmid DNA in MiaPaCa-2 cells utilizing nanovector delivery system.

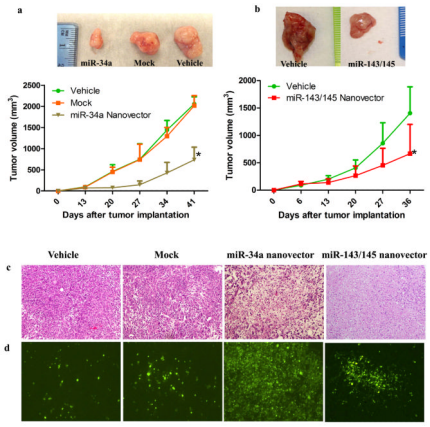

Figure 2. Systemic miRNA delivery with nanovectors inhibits the growth of subcutaneous pancreatic cancer xenografts

(a) Athymic mice bearing subcutaneous MiaPaCa-2 xenografts were treated with either vehicle control, "mock" nanovector (complexed with pMSCV only), or miR-34a nanovector (N = 5 mice per cohort), by tail-vein injection. Representative xenografts from each of the three cohorts are illustrated. Treatment with miR-34a nanovector significantly inhibited tumor growth ($P<0.01$), whereas “mock” nanovector showed comparable growth rate to vehicle control.

(b) Athymic mice bearing subcutaneous MiaPaCa-2 xenografts were treated with either vehicle control, or miR-143/145 nanovector (N = 5 mice per cohort), by tail-vein injection. Representative xenografts from both cohorts are illustrated. Treatment with miR-143/145 nanovector significantly inhibited tumor growth ($P<0.05$).

(c) Representative H&E stained tumor sections from vehicle, “mock” and treatment cohorts. Confluent necrotic areas were observed in xenografts treated with miR-34a and miR-143/145 nanovectors.

(d) Enhanced intra-tumoral apoptosis in the miRNA nanovector-treated xenografts is confirmed by TUNEL staining. Xenograft sections obtained from of miR-34a and miR-143/145 nanovector arms showed increased DNA fragmentation (*green*) compared with controls.

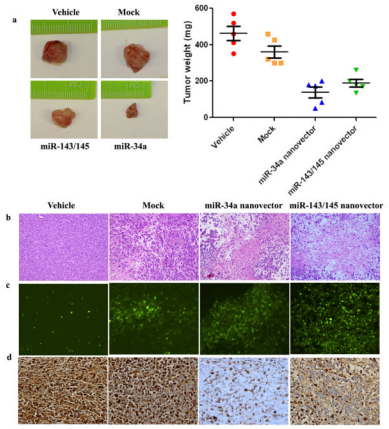

Figure 3. Systemic miRNA delivery with nanovectors inhibits the growth of orthotopic pancreatic cancer xenografts

(a) Athymic mice bearing orthotopic MiaPaCa-2 xenografts were treated with either vehicle control, "mock" nanovector, miR-34a nanovector, or miR-143/145 nanovector (N = 5 mice per cohort), by tail-vein injection. Representative xenografts from both cohorts are illustrated. Delivery of miR-34a and miR-143/145 nanovector significantly inhibited tumor growth ($p<0.0005$), whereas the “mock” nanovector showed comparable growth rate to vehicle control.

(b) Representative H&E stained tumor sections from vehicle, “mock” and treatment cohorts. Confluent necrotic areas were observed in xenografts treated with miR-34a and miR-143/145 nanovectors.

(c) Enhanced intra-tumoral apoptosis in the miRNA nanovector-treated xenografts was confirmed by TUNEL staining. Xenograft sections obtained from of miR-34a and miR-143/145 nanovector arms showed increased DNA fragmentation (*green*) compared with controls.

(d) Immunohistochemistry was performed for nuclear MIB-1 (Ki-67) antigen expression as a measure of cell proliferation. A reduction in Ki-67 labeling was observed in xenografts treated with miR-34a and miR-143/145 nanovectors, whereas no notable differences were observed between mice treated with "mock" nanovector and vehicle control.

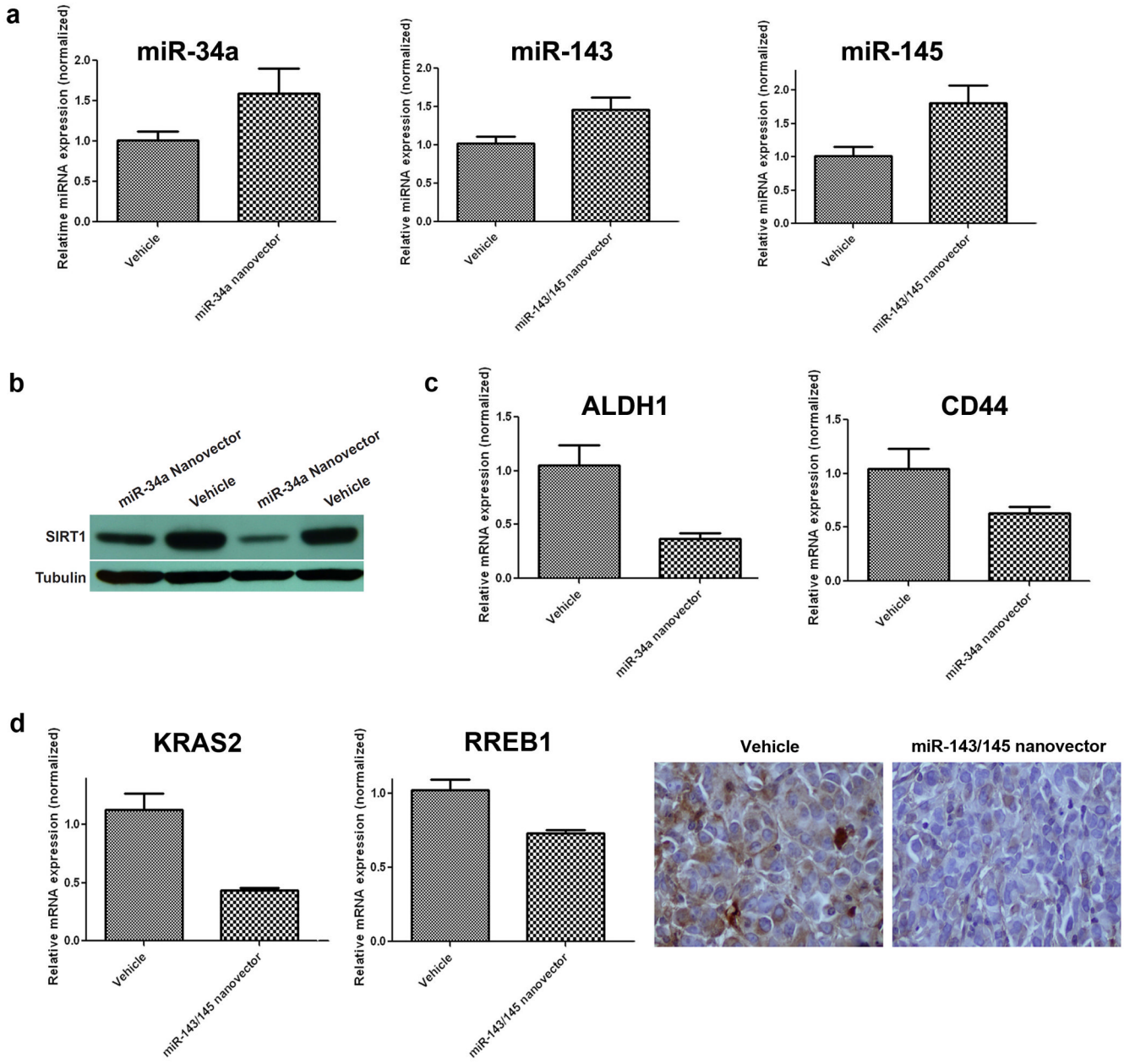

Figure 4. Systemic nanovector therapy modulates direct and indirect miRNA targets in pancreatic cancer xenografts

(a) Systemic miRNA delivery increased expression of the corresponding mature miRNA in treated MiaPaCa-2 xenografts. From left to right, relative levels are shown for miR-34a, miR-143 and miR-145 respectively, in nanovector-treated *versus* vehicle control xenografts. **(b)** Western blot analysis was performed to measure SIRT1, a direct target of miR-34a, in the miR-34a nanovector-treated xenografts. Reduction of SIRT1 expression was observed in the treatment *versus* vehicle xenografts (representative data is shown from two pairs), with tubulin used as a loading control.

(c) Systemic delivery of miR-34a significantly reduced expression of *aldehyde dehydrogenase (ALDH)* and *CD44* transcripts in treated *versus* vehicle control xenografts.

Cohorts of four independent xenografts were analyzed from each experimental condition, and *GAPDH* was used as an internal control.

(d) (*Left*) Systemic delivery of miR-143/145 significantly reduced expression of *KRAS2* and *RREB1* transcripts in treated *versus* vehicle control xenografts. Cohorts of four independent xenografts were analyzed from each experimental condition, and *GAPDH* was used as an internal control. (*Right*) Systemic delivery of miR-143/145 reduced expression of RREB1 protein in treated *versus* vehicle control xenografts. Cohorts of three independent xenografts were analyzed from treated versus control arms, and representative figures from one tumor in each cohort is illustrated.